Available online at www.sciencedirect.com
SCIENCE DIRECT®
Journal of Biotechnology xxx (2006) xxx–xxx
Journal of BIOTECHNOLOGY
www.elsevier.com/locate/jbiotec

Mechanical properties of single living cells encapsulated in polyelectrolyte matrixes

Tiziana Svaldo Lanero, Ornella Cavalleri, Silke Krol, Ranieri Rolandi, Alessandra Gliozzi *

Physics Department, University of Genoa, Via Dodecaneso 33, 16146 Genoa, Italy

Received 28 July 2005; received in revised form 19 January 2006; accepted 17 February 2006

Abstract

We have studied the mechanical properties of encapsulated *Saccharomyces cerevisiae* yeast cells by performing AFM force measurements. Single living cells have been coated through the alternate deposition of oppositely charged polyelectrolyte layers and mechanically trapped into a porous membrane. Coated and uncoated cells in presence/absence of bud scars, i.e. scars resulting from previous budding events, have been investigated. No significant differences between encapsulated and bare cells could be inferred from AFM topographs. On the other hand, investigation on the system elasticity through the acquisition and analysis of force curves allowed us to put in evidence the differences in the mechanical properties between the hybrid cell/polyelectrolyte system and the uncoated cells. Analysis of the curves contact region indicates that the polyelectrolyte coating increases the system rigidity. Quantitative evaluation of the cell rigidity through the Hertz–Sneddon model showed that coated cells are characterized by a Young's modulus higher than the value obtained for uncoated cells and similar to the value observed on the bud scar region of uncoated cells.

Keywords: Encapsulated cells; Young's modulus; AFM; Force spectroscopy; *Saccharomyces cerevisiae*

1. Introduction

Within the framework of new material research large interest is currently focussed on the design of hybrid cell/polyelectrolyte systems. The encapsulation of cells, single or in clusters, has potential impact in the biomedical field. The range of applications goes from suppression or reduction of the immunological response to transplants to the in situ targeting of encapsulated bioreactors for local drug production and delivery.

Several techniques have been exploited to produce cell coatings, from the use of alginates to prevent immune response in the transplant of pancreatic islets (e.g. de Vos et al., 2003) to the polyelectrolyte coating through layer-by-layer (L-by-L) deposition on living

* Corresponding author. Tel.: +39 010 3536221; fax: +39 010 314218.
E-mail address: gliozzi@mail.fisica.unige.it (A. Gliozzi).

0168-1656/$ – see front matter © 2006 Elsevier B.V. All rights reserved.
doi:10.1016/j.jbiotec.2006.02.016

single yeast cells or fungi (Diaspro et al., 2002; Krol et al., 2004). Firstly reported in 1997 (Decher, 1997) for the preparation of planar multilayers, the L-by-L technique has been successfully exploited for building up multilayer capsules on colloids (Sukhorukov et al., 1998). The method is based on the alternating deposition of oppositely charged polyelectrolytes onto charged cores: with or without subsequent core removal it ends up with empty or filled multilayer shells (Donath et al., 1998; Sukhorukov et al., 1998; Gao et al., 2000), with applications from pharmaceutics to cosmetics, and from food industry to cultural heritage conservation.

We focus here on the mechanical properties of encapsulated single living yeast cells to investigate how the coating can be used to tailor the system elastic properties. The coating is expected to increase the rigidity, thus leading to a hybrid system best suited to resist shear stress or other unfavourable environmental conditions. Moreover, investigations on the mechanical properties of the hybrid system could give better insight in the mechanism, which allows the cell to break the polyion capsule during duplication (Diaspro et al., 2002). To get information on the mechanical properties of coated cells, we performed force measurements using the atomic force microscope (AFM). Based on the measure of the local interaction between a sharp probe, placed at the apex of a cantilever, and the sample surface, AFM is a well-suited tool for the study of the morphology as well as the elastic properties of biological samples. Thanks to the possibility of working in liquid, i.e. in almost physiological conditions, AFM has been successfully used to image living cells (Henderson, 1994; Shao and Yang, 1995; Dufrêne, 2004). Additionally, AFM can be used to measure or apply small forces, enabling the study of cell mechanical properties (Radmacher, 1997). By approaching and retracting the AFM tip from the sample, it is possible to record a force versus distance curve, i.e. a plot of the cantilever deflection (from which the tip–sample force can be obtained) versus the piezo displacement (from which the tip–sample distance can be calculated) (Cappella and Dietler, 1999). The acquisition of matrixes of curves on different locations over a chosen sample area enables the mapping of the local mechanical properties (Heinz and Hoh, 1999). AFM has been successfully used to measure cellular nanomechanical motion due to cell metabolism (Pelling et al., 2004) and to follow furrow stiffening during division of adherent cells (Matzke et al., 2001). Mapping of the local elasticity of microbial cells has put in evidence stiffening of the cell wall in the bud scar region (Touhami et al., 2003).

As cellular system we used *Saccharomyces cerevisiae* culture stock, the common baker's yeast. It has been previously shown that the layer-by-layer technique can be successfully employed to encapsulate single *S. cerevisiae* cells which preserve their metabolic activity and duplication capability after encapsulation (Diaspro et al., 2002). Through the acquisition and analysis of force curves with the AFM we investigate the influence of the polyelectrolyte matrix on the yeast cell rigidity. The change in mechanical properties due to the coating is discussed and compared to the increase in cell rigidity related to duplication.

2. Materials and methods

2.1. Materials

S. cerevisiae cells from common baker's yeast were used as cellular system. They were coated by the alternate deposition of polycations and polyanions. For encapsulation, poly(styrene sulfonate sodium salt) (PSS, M_W 70,000 Da, Aldrich, Milan, Italy) and poly(allylamine hydrochloride) (PAH, M_W 15,000 Da, Aldrich, Milan, Italy) were dissolved in 0.5 M NaCl to a concentration of 2 mg/ml. Each PE layer was adsorbed by incubating the cells in the proper PE solution for 10 min; each adsorption step was followed by two washing steps in 0.5 M NaCl solution (centrifugation at 2000 rpm for 3 min) to remove the polyelectrolyte in excess. Four polyelectrolyte (PE) layers were assembled onto the cells.

2.2. AFM measurements

For reliable AFM measurements cells have to be anchored to a substrate; in this study mechanical trapping in a microporous membrane was used to immobilize encapsulated and uncoated cells in liquid (Kasas and Ikai, 1995). A suspension of cells was filtered through a polycarbonate membrane (Millipore, Milan, Italy) with pore size of ~5 μm close to the cell size (typical diameter 5–6 μm). Contact mode AFM images and force–distance curves were obtained at room temper-

ature, using a PicoForce/Nanoscope IV system (Digital Instruments, Santa Barbara, CA, USA) and Si_3N_4 cantilevers (DNP from Veeco; nominal spring constant of 0.06 N/m and nominal tip radius of 20–60 nm). For each cantilever, the spring constant was measured by the thermal noise method (Hutter and Bechhoefer, 1993) while the curvature radius of the tip was evaluated by using a silicon calibration grating with high aspect ratio spikes (TGT01, NT-MDT, Moscow, Russia). Mica was used as a rigid surface to calibrate photodetector sensitivity. All measurements were performed in 0.5 M NaCl solution. Force curves were recorded at a rate of 0.5 μm/s, with typical piezo displacements ranging from 600 nm to 1 μm. Force curves matrixes were obtained by the acquisition of an ensemble of curves (at least 50) on different locations regularly distributed over a chosen area of the cell surface. The analysis of the experimental curves was performed by using home made software developed in Fortran. Young's modulus values were obtained by the analysis of the contact region through the Hertz–Sneddon model (see Appendix A). The mean values of the Young's modulus were calculated as the average, weighted over the number of measurements, of the data obtained by the analysis of 230 curves from four independent experiments (coated cells), 209 curves from three independent experiments (uncoated cells without bud scar) and 250 curves from one experiment (uncoated cells with bud scar). Considering the mean values obtained on different cells, typical maximum relative deviations from the mean values are of about 20% for both coated and bare cells.

3. Results and discussion

Cell immobilization on a surface is a key step for reproducible AFM imaging. Mechanical trapping in a porous membrane is a non-invasive method to immobilize single living cells in liquid environment. Already reported for uncoated yeast cells (Kasas and Ikai, 1995; Pelling et al., 2004), the method is applied here to encapsulated cells. Fig. 1 shows an AFM image of an encapsulated yeast cell protruding from a pore in the polycarbonate membrane. AFM measurements performed on uncoated cells (data not shown) produce very similar results. At this resolution the cells are characterized by a homogeneous smooth surface and

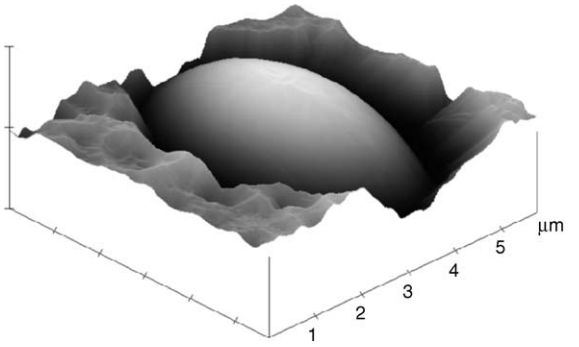

Fig. 1. 3D rendered AFM height image of an encapsulated cell trapped in a pore of a polycarbonate membrane in liquid ([NaCl] = 0.5 M); image size: 5.7 μm × 5.7 μm; z scale: 1 μm/div.

no difference between coated and uncoated cells can be detected from the AFM topographs.

As a comparative system, we have investigated the properties of uncoated cells with bud scars. Fig. 2 shows a cell with four circular regions, which are bud scars from previous cell divisions.

In order to investigate the mechanical properties of encapsulated and non-encapsulated cells, we recorded

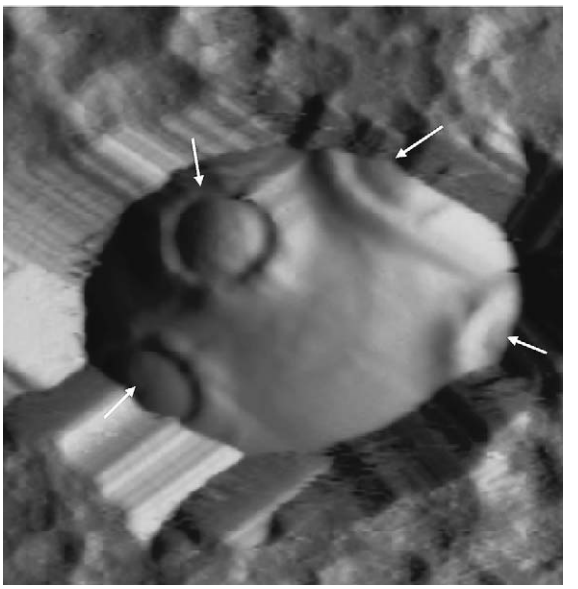

Fig. 2. Contact AFM deflection image of an uncoated multibud cell trapped in a pore of a polycarbonate membrane in liquid ([NaCl] = 0.5 M). The arrows indicate the multiple bud scars. The circular structured region around the cell is an artifact due to the interaction between the pore wall and the tip. Image size: 7.6 μm × 7.6 μm.

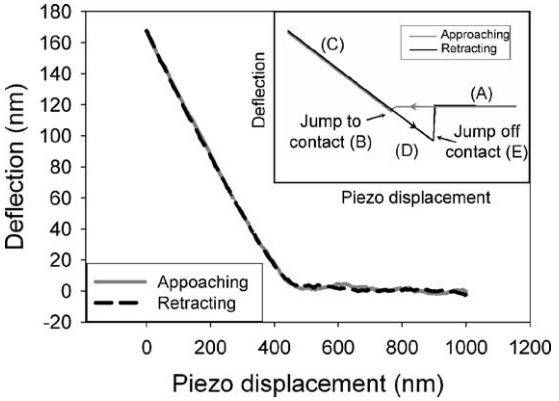

Fig. 3. Typical deflection vs. piezo displacement curve obtained on a coated yeast cell in liquid ([NaCl] = 0.5 M). Scan rate: 0.5 μm/s. Inset: generic deflection vs. piezo displacement curve (see Appendix A for a description).

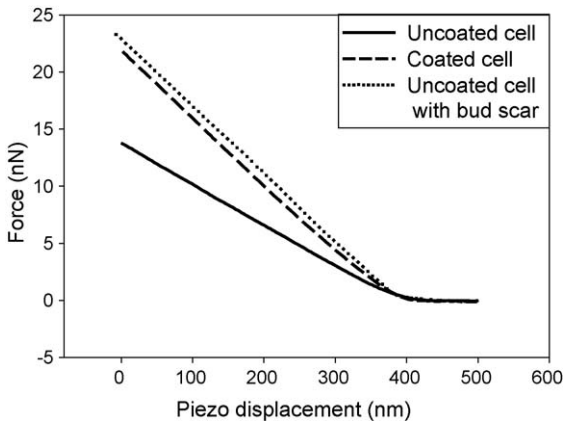

Fig. 4. Typical force vs. piezo displacement approaching curves for coated cells (dashed line), uncoated cells (solid line) and uncoated cells in the bud scar region (dotted line).

deflection versus piezo displacement curves. Since repeated curve acquisition on the same sample location could influence the sample properties, subsequent curves were recorded on different positions. Three different types of samples were analyzed: encapsulated cell, uncoated cell and uncoated cell with bud scars. A typical curve obtained on a coated cell is reported in Fig. 3. The absence of jump-to-contact is due to the electrostatic and osmotic repulsion (Butt, 1991) between the Si_3N_4 tip, whose surface has a negligible charge at pH ∼ 6 (Raiteri et al., 1996), and the coated cell, which is negatively charged due to the outermost PSS layer. The absence of jump-off-contact indicates that adhesion forces are negligible. The approaching and retracting curves, almost superimposed, indicate that the sample behaves elastically. We note that qualitatively similar curves are observed on uncoated cells. Deflection versus piezo displacement curves were transformed into force versus piezo displacement curves using the relation $F = k_c\delta_c$, where F is the load, k_c is the elastic constant of the cantilever and δ_c is the deflection. Typical approaching curves for the three considered systems are reported in Fig. 4: they present different slopes in the contact region. The slope of the contact region depends on the stiffness of the sample: a higher value of the modulus of the slope is associated to a stiffer surface. In fact, at a fixed piezo displacement, the stiffer the sample is, the less the tip indents the surface (i.e. the higher is the correspondent value of the cantilever deflection). From the comparison of the three curves in Fig. 4 it can be qualitatively inferred that, in a similar way as the bud scar does, the polyelectrolyte coating increases the cell rigidity.

To probe the homogeneity of the sample mechanical properties, matrixes of curves were acquired on a chosen area. The curves were processed in order to build up force maps, helpful for a better visualization of the spatial distribution of the elastic properties. The curves were superimposed at a fixed force value and cut at a chosen piezo displacement (Fig. 5b). The correspondent values of force f_i were used to make the maps. An example of force map obtained on a coated cell is reported in Fig. 5a: the sample mechanical properties are quite homogeneous over the examined area since no particular features are observed. Qualitatively similar results were obtained on uncoated cells without bud.

As discussed previously, both bare and coated cells behave elastically. For a quantitative evaluation of the system elasticity we have therefore analysed the force curves by using the Hertz–Sneddon model (see Appendix A). This model relates the load (force) exerted by an indenter, having a known shape, to the indentation depth of a sample, having a plane surface, under the hypothesis of an indenter Young's modulus much higher than the sample one and of no adhesion between indenter and sample. In our case the model conditions are fulfilled. The radius of the cells (>2.5 μm) is much larger than the radius of curvature of the tip (20–60 nm); therefore, in first approximation, the region of the cell involved in the contact process can

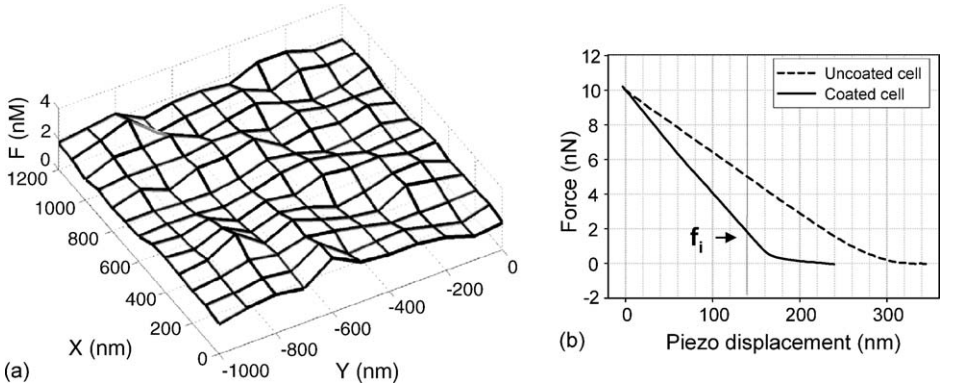

Fig. 5. (a) Force map obtained on a 1.2 μm × 1 μm region of a coated yeast cell by plotting the f_i values calculated by cutting the force curves, previously superimposed at a chosen force value (10 nN in this case), at a chosen piezo displacement (140 nm in this case) as shown in (b). According to this analysis stiffer samples are characterized by lower f_i values.

be considered plane with respect to the tip. The Young's modulus of the tip (E_{tip} = 150 GPa) is much higher than that of the sample. Since there is no jump-off-contact in the retracting curves, the adhesion between tip and sample is negligible. We note that in our case the sample is not a homogeneous material, but it has a complex structure (cell interior, cell membrane, cell wall and, for coated cells, polyelectrolyte coating). The Young's modulus value obtained through the Hertz model analysis has to be considered as an effective value relative to the whole system.

The Hertz–Sneddon equations (see Appendix A) link the load to the indentation depth while the experimental data consist in deflection versus piezo displacement curves. Deflection/piezo displacement curves can be changed into load/indentation curves by using the relations: $F = k_c\delta_c$ and $\delta = z - \delta_c$, where F is the load, k_c the elastic constant of the cantilever, δ_c the deflection of the cantilever, δ the indentation depth and z the piezo displacement (Weisenhorn et al., 1993). The model predicts that the load depends on the indentation according to a power law related to the tip geometry. In order to choose the correct tip geometry an equation of the form $F = a\delta^b$ was fitted to load versus indentation curves: based on the Hertz–Sneddon equations (Eqs. (1)–(3) in Appendix A) the exponent b depends on the tip shape. Since we obtained a value of b close to 3/2, characteristic of a spherical tip, the curves were fitted by using the spherical model (Fig. 6). Assuming a Poisson's ratio of 0.5 (expected for soft biological materials) and using the measured tip radius of curvature, we

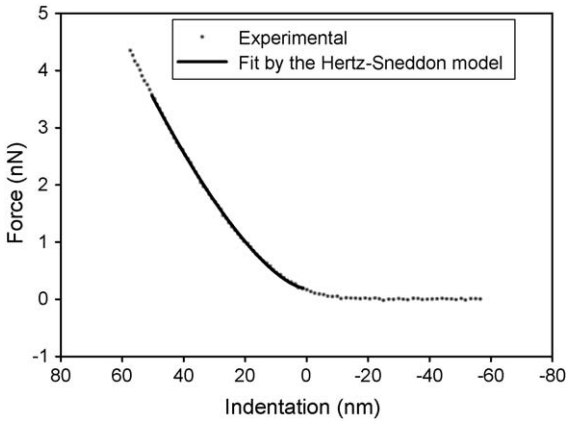

Fig. 6. Typical force vs. indentation curve of a coated yeast cell: experimental data (dotted line) and data generated using the Hertz–Sneddon model (solid line).

obtained Young's modulus values of 1.79 ± 0.08 MPa for encapsulated cells 1.12 ± 0.02 MPa for uncoated cells without bud scar and 2.0 ± 0.2 MPa for uncoated cells with bud scar (Table 1).

For uncoated cells, the data in literature (E = 0.6 ± 0.4 and 6.1 ± 2.4 Mpa for mother cell

Table 1
Mean values of the Young's modulus

Sample	Young's modulus (MPa)
Coated cell	1.79 ± 0.08
Uncoated cell	1.12 ± 0.02
Coated cell-bud scar	2.0 ± 0.2

and bud scar, respectively (Touhami et al., 2003)) report a higher rigidity of the bud scar compared to the mother cell. Our results are in qualitative agreement with those reported in literature even if a slightly lower value is obtained for bud scar. Several reasons could account for this discrepancy. The different yeast strain used and the different medium in which the measurements were performed could be partially responsible for the observed differences. Moreover, the bud scar value has been obtained as the average over a region "centered" on the bud scar. Because of possible drifts of the chosen region during the acquisition of the curve matrixes, contribution from mother cell regions around the bud scar cannot be excluded. Such contribution would lead to a lowering of the measured average stiffness compared to the "pure" bud scar stiffness.

Young's moduli in the range of MPa are in agreement with values reported in literature for bacterial cells (Yao et al., 1999; Touhami et al., 2003). The presence of a cell wall increases the cell rigidity compared to mammalian cells for which E values in the range of 0.1–100 kPa are reported (Radmacher, 2002).

Furthermore, the structure/composition of the cell wall largely influences the cell rigidity. AFM measurements on cell wall-defective mutants of *S. cerevisiae* indicate that modifying the cell wall composition by reducing the number of mannosylphosphate groups decreases the cell rigidity (Méndez-Vilas et al., 2004). In the present study, coating the cell wall with a PE matrix modifies the system's mechanical properties by increasing its rigidity.

It must be noted that the above cited papers as well as the present study investigate the cell elasticity through a local approach by using AFM. However the importance of the cell mechanical properties which play a key role in determining cell form and cell growth has prompted a number of investigations carried out by different techniques, from micropipette aspiration to osmotic swelling/shrinking, optical trapping and cell compression (Fung, 1993; Zahalak et al., 1990; Smith et al., 2000; Mendelson et al., 2000). These experimental techniques probe the elastic properties of the cell by applying a mechanical stress to the whole cell. Through a micromanipulation technique on *S. cerevisiae*, Middelberg and coworkers (Smith et al., 2000) obtained a Young's modulus of about 100 MPa and showed that yeast cells strengthen as they enter the stationary phase by increasing wall thickness without altering the average elastic properties of the cell-wall material. The large discrepancy between the elasticity data obtained by local and global techniques clearly indicates that different aspects of the cell elasticity are probed by the two approaches and further effort for a critical data comparison will be necessary.

To our knowledge, apart from a paper on dried coated cells (Yu and Ivanisevic, 2004), there are no data in literature about hydrated hybrid systems similar to those investigated in the present study. On the other hand, several papers have been published on the mechanical properties of polyelectrolyte multilayer capsules (for a review, Fery et al., 2004) investigated by colloidal AFM (Lulevich et al., 2003; Heuvingh et al., 2005) and by osmotically induced swelling experiments (Vinogradova et al., 2004; Gao et al., 2001a). Except for a colloidal AFM study (Lulevich et al., 2004) in which a value of 1–10 MPa (depending on the template) is given as a lower limit of the Young's modulus, Young's moduli in the range of hundreds of MPa are reported for capsules made by 8 up to 20 polyelectrolyte layers. Slight variations in the reported values were observed in dependence of the chosen polycation/polyanion couple, the core or the salt concentration of the medium. Young's moduli in the range of hundreds/thousands of MPa have been reported also for planar PSS/PAH multilayers in the wet/dry state (Nolte et al., 2005). The Young's modulus of polyelectrolyte capsules reported in literature are therefore higher than the Young's modulus of the hybrid polyelectrolyte/cell system investigated in the present paper. However no direct comparison of the two sets of values can be made since the values obtained here are not the Young's moduli of the polyelectrolyte coating alone, but are characteristic of the entire hybrid system. It is therefore reasonable that lower values are obtained. Moreover, in the present study we used a polycation with a molecular weight lower than the one usually reported in literature. Likely, the electrostatic interactions of short polycations with polyanions are weaker than those of long polycations. Actually an increase in the structure rigidity has been reported for hollow capsules prepared with high molecular weight polyelectrolytes (Dejugnat and Sukhorukov, 2004). In addition, for the hollow capsules templated on melamine formaldehyde, the significant quantity of remaining core material (Gao et al., 2001b) is likely to induce a stiffening of the capsule wall. The

aim of the present work was not the evaluation of the Young's modulus of the surface layer of coated cell, but mainly the comparison of the mechanical properties of coated and uncoated cells.

An interesting point which deserves further investigations concerns the interactions between the cell and the adsorbed polyelectrolyte layer: the use of a living cell as a template is likely to make the mechanism of PE assembly more complex when compared to the coating of polymer cores or ionic crystals. It is reasonable to suppose that living cells can react to an external perturbation, like the PE coating. Some hints for this hypothesis come from a previous study on the immobilization of encapsulated living cells on patterned surfaces: while cells encapsulated with a negatively terminated coating selectively adsorb on positively charged patterns, no selective adsorption (on negatively charged patterns) is achieved when using cells encapsulated with a positively terminated coating (Krol et al., 2005). This suggests that living cells are able to actively change the surface charge of the attached polyelectrolyte layers and deserves further quantitative analysis of the surface charge density of the coated cells as a function of the outermost layer. Such an "active" cell role is likely to affect the mechanical properties of the PE multilayers as well. It will be therefore interesting to evaluate the Young's modulus of the PE cell coating and to compare it to the values obtained for PE layers assembled on inorganic cores.

Work is in progress as well to address the dependence of the Young's modulus of coated cells on the thickness of the polyelectrolyte coating and to investigate the influence of the coating rigidity on the cell duplication capability.

Acknowledgements

Financial support from MIUR (contract no. 2003028141-005) is acknowledged. S.K. was supported by the EC contract BARP+: NMP3-CT-2003-505614.

Appendix A

A generic cantilever deflection versus piezo displacement curve is reported in the inset of Fig. 3. At large tip–sample distances (A) there is no interaction between tip and sample and the cantilever is not deflected. During the approach, the tip is suddenly captured by the sample (jump-to-contact) (B). Approaching further, we move in the contact region (C). Upon reversal of the piezo movement direction, the tip is retracted from the sample (D) until the jump-off-contact (E) is observed and the tip is released from the surface. The analysis of the contact region gives information on the sample elastic properties: if the sample behaves elastically approaching and retracting curves are superimposed while a hysteresis indicates a plastic behaviour. The absence of the jump-to-contact indicates the presence of repulsive forces balancing attractive van der Waals forces. A large jump-off-contact is due to adhesive forces set up in the contact region.

The Hertz–Sneddon model. In the contact region, the behaviour of the cell–tip–cantilever system can be described by the continuum mechanics of elastic contact. The model describes the behaviour of a known geometry indenter in contact with an elastic half-space much less rigid than the punch (Sneddon, 1965). In the Hertz–Sneddon equations the load exerted by the punch is linked to the caused indentation depth. In the application to the AFM measurements the generally considered indenter's geometries are the conical, the paraboloidal and the cylindrical ones (Weisenhorn et al., 1993):

$$F_{\text{cone}} = \frac{2}{\pi} tg\alpha \frac{E}{1-\nu^2}\delta^2 \quad (1)$$

$$F_{\text{paraboloid}} = \frac{4}{3}\frac{E}{1-\nu^2} R^{1/2}\delta^{3/2} \quad (2)$$

$$F_{\text{cylindre}} = 2\frac{E}{1-\nu^2} a\delta \quad (3)$$

where F is the load exerted by the tip, E the Young's modulus and ν the Poisson's ratio of the elastic half-space, α the half-opening angle of a conical tip and R is the radius of curvature of a paraboloidal or a spherical tip and a the radius of a cylindrical tip.

These models describe the contact between an elastic sample with a planar contact surface and a rigid punch under the hypothesis of negligible adhesion between tip and sample.

References

Butt, H.-J., 1991. Electrostatic interaction in atomic force microscopy. Biophys. J. 60, 777–785.

Cappella, B., Dietler, G., 1999. Force–distance curves by atomic force microscopy. Surf. Sci. Reports 34, 1–104.

Decher, G., 1997. Fuzzy nanoassemblies: toward layered polymeric multicomposites. Science 277, 1232–1237.

Dejugnat, C., Sukhorukov, G., 2004. pH-responsive properties of hollow polyelectrolyte microcapsules templated on various cores. Langmuir 20, 7265–7269.

de Vos, P., van Hoogmoed, C.G., van Zanten, J., Netter, S., Strubbe, J.H., Busscher, H.J., 2003. Long-term biocompatibility, chemistry, and function of microencapsulated pancreatic islets. Biomaterials 24, 305–312.

Diaspro, A., Silvano, D., Krol, S., Cavalleri, O., Gliozzi, A., 2002. Single living cell encapsulation in nano-organized polyelectrolyte shells. Langmuir 18, 5047–5050.

Donath, E., Sukhorukov, G.B., Caruso, F., Davis, S., Möhwald, H., 1998. Novel hollow polymer shells by colloid-templated assembly of polyelectrolytes. Angew. Chem. Int. Ed. 37, 2201–2205.

Dufrêne, Y.F., 2004. Using nanotechniques to explore microbial surfaces. Nat. Rev. Microbiol. 2, 451–460.

Fery, A., Dubreil, F., Möhwald, H., 2004. Mechanics of artificial microcapsules. New J. Phys. 6 (art. no. 18).

Fung, Y.C., 1993. Biomechanics: Mechanical Properties of Living Tissues, second ed. Springer, New York.

Gao, C., Leporatti, S., Donath, E., Möhwald, H., 2000. Surface texture of poly(styrenesulfonate sodium salt) and poly(diallyldimethylammonium chloride) micron-sized multilayer capsules: a scanning force and confocal microscopy study. J. Phys. Chem. B 104, 7144–7149.

Gao, C., Leporatti, S., Moya, S., Donath, E., Möhwald, H., 2001a. Stability and mechanical properties of polyelectrolyte capsules obtained by stepwise assembly of poly(styrenesulfonate sodium salt) and poly(diallyldimethylammonium) chloride onto melamine resin particles. Langmuir 17, 3491–3495.

Gao, C.Y., Moya, S., Lichtenfeld, H., Casoli, A., Fiedler, H., Donath, E., Mohwald, H., 2001b. The decomposition process of melamine formaldehyde cores: the key step in the fabrication of ultrathin polyelectrolyte multilayer capsules. Macromol. Mater. Eng. 286, 355–361.

Heinz, W.F., Hoh, J.H., 1999. Spatially resolved force spectroscopy of biological surfaces using the atomic force microscope. Tibtech 17, 143–150.

Henderson, E., 1994. Imaging of living cells by atomic force microscopy. Prog. Surf. Sci. 46, 39–60.

Heuvingh, J., Zappa, M., Fery, A., 2005. Salt softening of polyelectrolyte multilayer capsules. Langmuir 21, 3165–3171.

Hutter, J.L., Bechhoefer, J., 1993. Calibration of atomic force microscope tips. Rev. Sci. Instrum. 64, 1868–1873.

Kasas, S., Ikai, A., 1995. A method for anchoring round shaped cells for atomic force microscope imaging. Biophys. J. 68, 1678–1680.

Krol, S., Diaspro, A., Magrassi, R., Ballario, P., Grimaldi, B., Filetici, P., Ornaghi, P., Ramoino, P., Gliozzi, A., 2004. Nanocapsules: coating for living cells. IEEE Trans. Nanobiosci. 3, 32–38.

Krol, S., Nolte, M., Diaspro, A., Mazza, D., Magrassi, R., Gliozzi, A., Fery, A., 2005. Encapsulated living cells on microstructured surfaces. Langmuir 21, 705–709.

Lulevich, V.V., Radtchenko, I.L., Sukhorukov, G.B., Vinogradova, O.I., 2003. Mechanical properties of polyelectrolyte microcapsules filled with a neutral polymer. Macromolecules 36, 2832–2837.

Lulevich, V.V., Andrienko, D., Vinogradova, O.I., 2004. Elasticity of polyelectrolyte multilayer microcapsules. J. Chem. Phys. 120, 3822–3826.

Matzke, R., Jacobson, K., Radmacher, M., 2001. Direct, high-resolution measurement of furrow stiffening during division of adherent cells. Nat. Cell Biol. 3, 607–610.

Mendelson, N.H., Sarlls, J.E., Wolgemuth, C.W., Goldstein, R.E., 2000. Chiral self-propulsion of growing bacterial macrofibers on a solid surface. Phys. Rev. Lett. 84, 1627–1630.

Méndez-Vilas, A., Corbacho, I., González-Martín, M.L., Nuevo, M.J., 2004. Direct surface probing of cell-wall defectve mutants of *Saccharomyces cerevisiae* by atomic force microscopy. Appl. Surf. Sci. 238, 51–63.

Nolte, A.J., Rubner, M.F., Cohen, R.E., 2005. Determining the Young's modulus of polyelectrolyte multilayer films via stress-induced mechanical buckling instabilities. Macromolecules 38, 5367–5370.

Pelling, A.E., Sehati, S., Gralla, E.B., Valentine, J.S., Gimzewski, J.K., 2004. Local nanomechanical motion of the cell wall of *Saccharomyces cerevisiae*. Science 305, 1147–1150.

Radmacher, M., 1997. Measuring the elastic properties of biological samples with the AFM. IEEE Eng. Med. Biol. 16 (2), 47–57.

Radmacher, M., 2002. Measuring the elastic properties of living cells by AFM. Methods Cell Biol. 68, 67–84.

Raiteri, R., Martinoia, S., Grattarola, M., 1996. pH-dependent charge density at the insulator-electrolyte interface probed by a scanning force microscope. Boisens. Bioelectron. 11, 1009–1017.

Shao, Z., Yang, J., 1995. Progress in high resolution atomic force microscopy in biology. Q. Rev. Biophys. 23, 115–139.

Smith, A.E., Zhang, Z., Thomas, C.R., Moxham, K.E., Middelberg, A.P.J., 2000. The mechanical properties of *Saccharomyces cerevisiae*. Proc. Nat. Acad. Sci. U.S.A. 29, 9871–9874.

Sneddon, I.N., 1965. The relation between load and penetration in the axisymmetric boussinesq problem for a punch of arbitrary profile. Int. J. Eng. Sci. 3, 47–57.

Sukhorukov, G.B., Donath, E., Lichtenfeld, H., Knippel, E., Knippel, M., Budde, A., Möhwald, H., 1998. Layer-by-layer self-assembly of polyelectrolytes on colloidal particles. Coll. Surf. A 137, 253–266.

Touhami, A., Nysten, B., Dufrêne, Y.F., 2003. Nanoscale mapping of the elasticity of microbial cells by atomic force microscopy. Langmuir 19, 4539–4543.

Yao, X., Jericho, M., Pink, D., Beveridge, T., 1999. Thickness and elasticity of Gram-Negative Murein Sacculi measured by atomic force microscopy. J. Bacteriol. 181, 6865–6875.

Yu, M., Ivanisevic, A., 2004. Encapsulated cells: an atomic force microscopy study. Biomaterials 25, 3655–3662.

Vinogradova, O.I., Adrienko, D., Lulevich, V.V., Nordschild, S., Sukhrukov, G.B., 2004. Young's modulus of polyelectrolyte

multilayers from microcapsule swelling. Macromolecules 37, 1113–1117.

Weisenhorn, A.L., Khorsandi, M., Kasas, S., Gotzos, V., Butt, H.J., 1993. Deformation and height anomaly of soft surfaces studied by an AFM. Nanotechnology 4, 106–113.

Zahalak, G.I., McConnaughey, W.B., Elson, E.L., 1990. Determination of cellular mechanical properties by cell pocking, with an application to leukocytes. J. Biomech. Eng. 112, 283–294.